

APPLICATION OF MULTISOURCE DATA FOR URBAN LAND COVER MAPPING

D.Amarsaikhan

Institute of Informatics and RS, Mongolian Academy of Sciences, av.Enkhtaivan-54B, Ulaanbaatar-51, Mongolia
amar64@arvis.ac.mn

KEY WORDS: Optical data, InSAR data, Rule-based method, Urban mapping

ABSTRACT:

The aim of this study is to discriminate urban land cover types using the features derived from optical and spaceborne interferometric synthetic aperture radar (InSAR) data sets. For the efficient discrimination of the selected classes, a rule-based algorithm that uses the initial image segmentation procedure based on a Mahalanobis distance rule and the constraints on spectral parameters and spatial thresholds is constructed. The result of the rule-based method is compared with the results of a standard supervised classification and it demonstrates a higher accuracy. Overall, the research indicates that the integrated features of the optical and InSAR images can significantly improve the classification of land cover types and the rule-based classification is a powerful tool in the production of a reliable land cover map.

1. INTRODUCTION

As it is known, remote sensing (RS) images taken in the optical range of the electro-magnetic spectrum contain information on the reflective and emissive characteristics of the Earth surface features, while the synthetic aperture radar (SAR) images (intensity and coherence) contain information on the surface roughness, texture, dielectric properties and change of the state of natural and man-made objects. In years past, the integrated features of these multisource data sets have been efficiently used for an improved land cover mapping. It is evident that a combined use of the optical and SAR images will have a number of advantages because a specific object or class which is not seen on the passive sensor image might be seen on the active sensor image and vice versa because of the nature of the used electro-magnetic radiation (Amarsaikhan 2000, Amarsaikhan *et al.* 2004).

Optical RS data sets taken from different Earth observation satellites such as Landsat and SPOT have been successfully used for land cover mapping since the operation of the first Landsat launched in 1972, whereas SAR images taken from space platforms have been widely used for different thematic applications since the launch of the ERS-1/2, JERS-1 and RADARSAT satellites (Amarsaikhan *et al.* 2004). The combined application of data sets from both sources can provide unique information for different thematic studies, because passive sensor images will represent spectral variations of various surface features, whereas microwave data with its penetrating capabilities can provide some additional information. For example, in urban context the optical images provide the information about the spectral variations of the urban features, whereas the radar images provide structural information about buildings and street alignment due to the double bounce scattering (Amarsaikhan and Douglas, 2004).

In general, urban areas include complex and diverse environment, in which many features have similar spectral characteristics and it is not easy to separate them by the use of ordinary feature combinations or by applying standard techniques. In the present study, we wanted to discriminate urban land cover types using the features derived from optical

and InSAR data sets. As a test site, Ulaanbaatar, the capital city of Mongolia has been selected. The data used consisted of ERS-1/2 tandem pass SAR images, JERS-1 SAR intensity image and a SPOT XS image of 1997. For the efficient discrimination of the selected classes from the multisource images, a rule-based algorithm has been constructed. The constructed rule-based approach consists of a set of rules, which contains the initial image segmentation procedure based on the Mahalanobis distance classifier and the constraints on spectral parameters and spatial thresholds. In the Mahalanobis distance classifier, the features extracted through a feature extraction process, were used. As the reliable features in which the selected classes could be more separable, the principal component (PC)s extracted through the principal component analysis (PCA) have been chosen. The PCA has been performed using 6 bands, including the SPOT XS and SAR products. Overall, the research indicated that the integrated features of the optical and InSAR images can significantly improve the classification of land cover types and the rule-based classification is a powerful tool in the production of a reliable land cover map.

2. STUDY AREA AND DATA SOURCES

As a test site, Ulaanbaatar, the capital city of Mongolia has been selected. Ulaanbaatar is situated in the central part of Mongolia, on the Tuul River, at an average height of 1350m above sea level and currently has nearly 900,000 inhabitants (Mongolian Statistical Year Book, 2005). The selected part of the capital city is about 13.2kmx9.8km and is characterized by such classes as buildings, gers (Mongolian national dwelling), forest, vegetation, soil and water.

The data used consisted of C-band (wavelength is 5.66cm) ERS-1/2 tandem pass (interferometric) SAR single look complex (SLC) images acquired on 10 and 11 October 1997 with a spatial resolution of 25m, L-band (wavelength is 23.5cm) JERS-1 SAR intensity image of April 1997 with a spatial resolution of 18m and a SPOT XS image of 19 June 1997 with a spatial resolution of 20m. In addition, for ground truth checking a topographic map of 1984, scale 1:50,000 and a general urban planning map were available. Figure 1 shows the

test area in a SPOT XS image and some examples of its land cover.

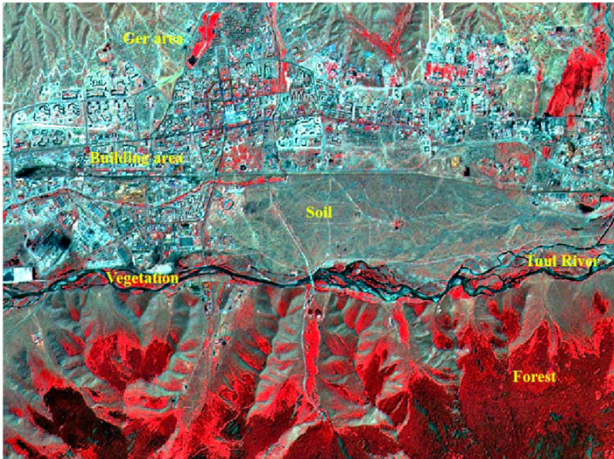


Figure 1. SPOT XS image of the selected part of Ulaanbaatar (Red=band3, Green=band2, Blue=band1). The size of the displayed area is about 13.2kmx9.8km.

3. DERIVATION OF THE ORTHORECTIFIED AND INSAR COHERENCE IMAGES

The main goal in orthorectification is to determine, for a given location on the Earth's surface, the associated range line and range pixel from the input SAR image, including the terrain effects. Generally, orthorectified SAR images are derived from the original SLC SAR images. For the terrain correction (eg, correcting the lay-over effects produced by radar imagery), a digital elevation model (DEM) is used.

In the present study, initially, an interferometric DEM has been derived from a pair of ERS-1/2 tandem pass SAR SLC images using the IFSAR module of the ERDAS Imagine. Then, an orthorectified ERS SAR image has been derived using the OrthoRadar module of the ERDAS system. For the terrain correction, the previously derived interferometric DEM was used.

The InSAR coherence images are generated by using both the amplitude and phase information from a pair of SLC images. The coherence is a measure of the variance of the phase difference of the imaged surface in the time between the two SAR data acquisitions. The coherence values range between 0 and 1. If some land surface changes had occurred in a target area between the two image acquisition periods, then coherence is low and if no changes had occurred, then the coherence is high (Weydahl, 2001). In general, the coherence over a dense forest and shrub will be the lowest, while for the bare soil, the coherence will be the highest. Using the BEST (BEST, 2005) software, the coherence image has been derived as follows:

1. Initially, 200 ground control points (GCP) regularly distributed over the images were automatically defined using the satellite orbit parameters and the two SLC images were co-registered with 0.1pixel accuracy. Then, a course registration followed by a fine registration was performed.
2. Coherence has been calculated using 15x3 size window and the coherence image was generated.

3. The preliminary SLC images were converted from the slant range onto a flat ellipsoid surface.
4. The true size (5800x5800) image was generated using image undersampling by applying a 3x3 size low pass filter.

4. DERIVATION OF THE TEXTURE FEATURES OF THE SAR PRODUCTS

To derive the texture features of the SAR products, occurrence and co-occurrence measures were applied to the coherence and ERS SAR as well as JERS-1 SAR intensity images. The occurrence measures use the number of occurrences of each grey level within the processing window for the texture calculations, while the co-occurrence measures use a grey-tone spatial dependence matrix to calculate texture values (ENVI, 1999). By applying these measures, initially 40 features have been obtained, but after thorough checking of each individual feature only 8 features including the results of the mean and data range filters applied to all three images, and the results of the variance filter applied to the ERS and JERS-1 intensity images were selected.

5. COREGISTRATION OF THE MULTISENSOR IMAGES

Initially, the SPOT image was geometrically corrected to a Gauss-Kruger map projection using a topographic map of the study area, scale 1:50,000. The GCPs have been selected on clearly delineated crossings of roads, streets, rivers and other clear sites. In total 16 points were selected. For the transformation, a second order transformation and nearest neighbour resampling approach have been applied and the related root mean square (RMS) error was 0.86 pixel. In order to correct the coherence and JERS-1 SAR images, 24 more regularly distributed GCPs were selected comparing the locations of the selected points with other information such as SPOT XS image and the topographic map. Then, the images were geometrically corrected to a Gauss-Kruger map projection using the topographic map of the study area. For the actual transformation, a third order transformation and nearest neighbour resampling approach were applied and the related RMS errors were 0.97 pixel and 0.94 pixel for the coherence product and JERS-1 SAR image, respectively.

6. EVALUATION OF THE FEATURES USING A SUPERVISED CLASSIFICATION METHOD

Generally, before applying a classification decision rule, the speckle noise of the SAR images should be reduced. The reduction of the speckle increases the spatial homogeneity of the classes, which in turn improves the classification accuracy. Initially, in order to reduce the speckle of the radar images, a 3x3 gammamap filtering (Gonzalez and Woods, 2002) was applied to the JERS-1 SAR and ERS SAR products. Then, from the multisource images, 2-3 areas of interest (AOI) representing the selected six classes such as building area, ger area, forest, vegetation, soil and water have been selected through accurate analysis using a polygon-based approach. The separabilities of the training signatures were firstly checked on the feature space images and then evaluated using JM distance (Richards, 1993). Then the samples which demonstrated the greatest separabilities were chosen to form the final signatures. The final signatures included about 86-594 pixels.

For the evaluation of the selected feature combinations, the standard statistical maximum likelihood classifier has been used assuming that the training samples have the Gaussian distribution (Mather, 1999). For the classification, the following feature combinations have been used:

1. The SPOT XS and ERS SAR
2. The SPOT XS and coherence
3. The SPOT XS and JERS-1 SAR
4. The SPOT XS, coherence and ERS SAR
5. The SPOT XS, JERS-1, coherence, ERS SAR
6. Multiple features, including the original SPOT XS and SAR products as well as 8 texture features determined through occurrence and co-occurrence measures
7. The first 6 principal components (PC) of the principal component analysis (PCA) (Richards 1993). The PCA was performed using multiple (14) features.

The images classified by each of the above mentioned feature combinations are shown in Figure 2(a-g). For the accuracy assessment of the classification results, the overall performance has been used (ERDAS, 1999). As ground truth information, for each class several regions containing the purest pixels have been selected. The overall classification accuracies for the selected classes are shown in Table 1.

As seen from Figure 2 (a-g) and Table 1, compared to other results the classification accuracy of combination of the SPOT XS and coherence image is not high. In urban context, coherence cannot add much information, but it might have some contribution to separate the fuzzy boundaries between green vegetation and forest, because as the state of the vegetation is more stable than that of forest, it would result in higher coherence values than forest. However, it is seen that a combination of the SPOT XS with either JERS-1 or original ERS products gave improved classification results. Specifically, the combination of the XS and JERS-1 images gave better result in terms of separation among the statistically overlapping classes such as building area, ger area and soil. This is most probably, due to the nature of the longer wavelength of JERS-1 which can totally separate backscatter of soil that has specular reflection from the backscatter of urban or forest classes which are dominated by double bounce and volume scattering, respectively. Moreover, it is seen that the classification result of combination of the SPOT XS and original SAR products is the highest among the selected feature combinations. This indicates that multisource information collected from optical as well as different radar frequencies can significantly improve the classification result, however, using a standard technique it is very difficult to obtain the most reliable result.

Furthermore, as seen from Figure 2 (a-g) and Table 1, the accuracy of the classification result of the created 14 features is not high. This is probably due to the influence of texture features whose variances make confusions in decision boundaries in multidimensional space. Likewise, the accuracy of the PC bands is not high, too. When the PCA was performed to 14 features, it is interesting to notice that the first 3 PCs were dominated by the variance of the SAR texture features and contained 99.78% of the overall data variance. When they were classified, the result was not reliable, because they contained different mixed classes. Further inspection of the PCs indicated that PC4 was dominated by the variance of the visible bands of the SPOT XS, while PC5 was dominated by the variance of the

original SAR bands. The inspection of other PCs indicated that PC6 was dominated by the variance of the infrared band of the SPOT XS and the rest contained noise from the total data set. Therefore, for the classification the first 6 PCs which contained 99.98% of the total data variance were used. As seen from the classification result of the PC images, there are different mixed classes. This is probably because of the influences of the texture features.

As seen, although the multisource data sets produced better results, they could not separate the two statistically overlapping urban classes such as building area and ger area. An attempt to separate these classes will be made in the next section, which describes a rule-based classification method.

The feature combinations used for the MLC	Overall accuracy (%)
SPOT XS and ERS SAR	84.12
SPOT XS and coherence	70.09
SPOT XS and JERS-1	84.86
SPOT XS, coherence and ERS	81.16
SPOT XS, JERS-1, coherence and ERS	88.87
Multiple features, including the original SPOT XS and SAR products as well as 8 texture features	79.91
The first 6 PCs of the PCA	74.56

Table 1. The overall classification accuracy of the classified images.

7. RULE-BASED CLASSIFICATION

Over the years, knowledge-based techniques have been widely used for the digital classification of RS images. The knowledge in image classification can be represented in different forms depending on the type of knowledge and necessity of its usage (Amarsaikhan and Douglas, 2004).

The most commonly used techniques for knowledge representation are a rule-based approach and neural network classification (Amarsaikhan 2000). In the present study, for separation of the statistically overlapping classes, a rule-based approach has been used. A rule-based approach uses a hierarchy of rules, or a decision tree describing the conditions under which a set of low level primary objects gets abstracted into a set of the high level object classes. The primary objects contain the user-defined variables and include geographical objects represented in different structures, external programmes, scalars and spatial models (ERDAS, 1999). The constructed rule-based approach consists of a set of rules, which contains the initial image segmentation procedure based on a Mahalanobis distance classifier and the constraints on spectral parameters and spatial thresholds. The Mahalanobis distance classifier is a parametric method, in which the criterion to determine the class membership of a pixel is the minimum Mahalanobis distance between the pixel and the class centre.

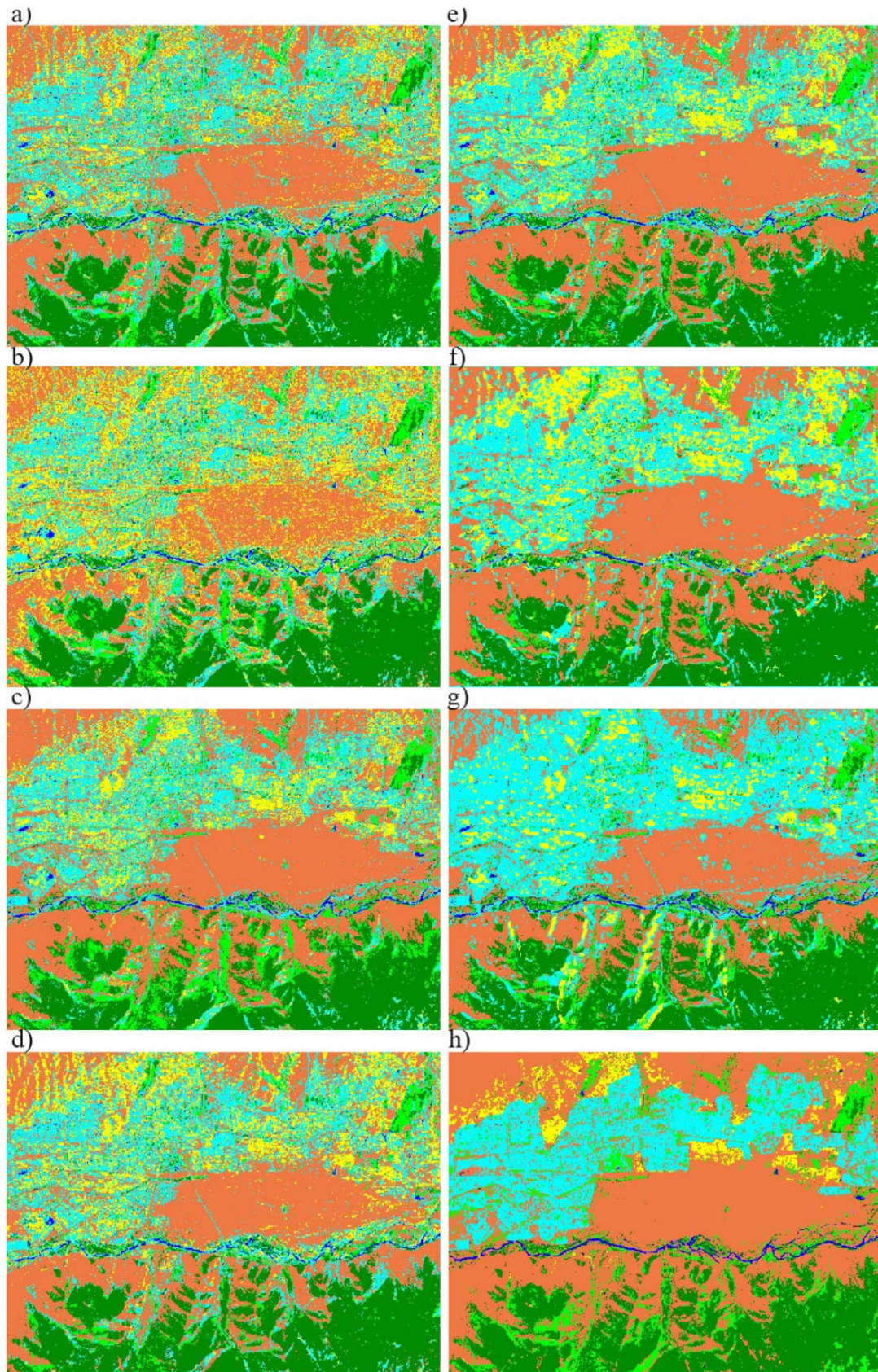


Figure 2. Comparison of the classification results for the selected classes (urban area-cyan, ger area-yellow, forest-dark green, vegetation-green, soil-brown, water-blue), (a) Classified image using SPOT XS and ERS, (b) Classified image using SPOT XS and coherence, (c) Classified image using SPOT XS and JERS-1 SAR, (d) Classified image using SPOT XS, coherence and ERS, (e) SPOT XS, JERS-1, coherence and ERS, (f) Multiple features, (g) Classified image using the first 6 PCs of the PCA, (h) Result of the rule-based method.

The Mahalanobis distance (MD_k) is expressed as follows:

$$MD_k = (x_i - m_k)^t V_k^{-1} (x_i - m_k) \quad (1)$$

where x_i is the vector representing the pixel, m_k is the sample mean vector for class k , and V_k is the sample variance-covariance matrix of the given class.

In the Mahalanobis distance estimation, for the initial separation of the classes, only pixels falling within 1.5 standard deviation (SD) and the features extracted through a feature extraction process, were used. As the reliable features in which the selected classes could be more separable, the PCs extracted through the PCA have been chosen. The PCA has been performed using 6 bands, including the SPOT XS and SAR products. The result is shown in Table 2.

As seen from Table 2, in the PC1 that contains 39.46% of the overall variance, JERS-1 has a very high negative loading, whereas in the PC2 that contains 31.23% of the overall variance, variance of the visible green band of SPOT XS has a total dominance. In the PC3 that contains 17.68% of the overall variance, coherence has a very high negative loading and further visual inspection revealed that this feature contained less information related to the selected classes. Moreover, as seen from the Table 2, in the PC4 that contains 8.83% of the overall variance, infrared band of the SPOT XS has a very high negative loading. The inspection of the last 2 PCs indicated that they contained noise from the total data set. As the PC3 had less information in terms of describing the selected classes, for the final features, PC1, PC2 and PC4 have been chosen. For the initial image segmentation, these selected features were evaluated using a Mahalanobis distance estimation.

The pixels falling outside of 1.5 SD were temporarily identified as unknown classes and further classified using the rules in which different spectral and spatial thresholds were used. The spectral thresholds were determined based on the knowledge about spectral and scattering characteristics of the selected six classes, whereas the spatial thresholds were determined using polygon boundaries separating the overlapping classes. The flowchart for the constructed rule-based approach is shown in Figure 3 and the image classified by this method is shown in Figure 2h. As seen from the image, the rule-based approach could very well separate the building area from the ger area compared to the results obtained by the maximum likelihood classifier. The overall classification accuracy has been evaluated using the same set of regions containing the purest pixels as in the previous classification and it demonstrated an improvement to 95.16%.

	PC1	PC2	PC3	PC4	PC5	PC6
XS1	0.026	0.981	-0.064	0.092	0.092	-0.019
XS2	0.048	0.104	0.171	0.002	-0.976	-0.032
XS3	0.036	0.091	-0.034	-0.992	0.002	-0.081
Coherence	-0.540	-0.051	-0.821	0.002	-0.176	0.002
ERS SAR	0.021	0.028	-0.006	-0.076	-0.028	0.996
JERS-1	-0.841	0.015	0.541	-0.051	0.053	0.016
Eigenvalue	6434.6	5095.2	2883.3	1440.3	355.5	103.1
Variance %	39.46	31.23	17.68	8.83	2.18	0.62

Table 2. Principal component coefficients from the SPOT XS and original SAR features.

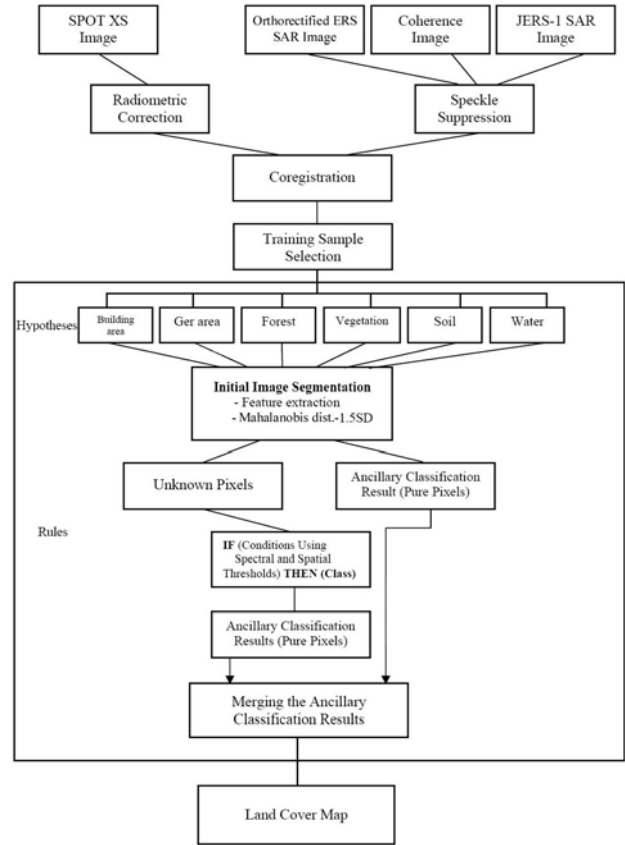


Figure 3. A general diagram for the rule-based classification.

8. CONCLUSIONS

The aim of the study was to discriminate the urban land cover classes using the features extracted from optical and spaceborne InSAR data sets. The initial multisource data sets included ERS-1/2 tandem pass SAR images, JERS-1 SAR intensity image and SPOT XS data of the urban area in Mongolia. In the feature derivation process, coherence and other texture features were derived from the SAR data.

For the efficient classification of the selected classes, a rule-based algorithm that uses the initial image segmentation procedure based on a Mahalanobis distance classifier and the constraints on spectral parameters and spatial thresholds were constructed. The result of the constructed rule-based algorithm was compared with the results of a standard maximum likelihood classification and it demonstrated a higher accuracy.

Overall, the research demonstrated that the integrated features of the optical and InSAR images can significantly improve the classification of land cover types and the rule-based classification is a powerful tool in the production of an accurate land cover map that can be directly used for a decision-making process.

ACKNOWLEDGEMENT

The author is grateful for having been selected as the Best ITC Alumni paper submitted to the Symposium, awarded by ITC's Directorate as part of ITC's 55th Anniversary celebrations and for the financial support to attend the Symposium.

REFERENCES

Amarsaikhan, D. and Ganzorig, M., 1997. Comparison of different pattern recognition techniques. Scientific Papers of Informatics Centre, Mongolian Academy of Sciences, pp. 71-75.

Amarsaikhan, D., 2000. Application of spectral and scattering knowledge for interpretation of active and passive sensor data. Institute of Informatics and RS, Mongolian Academy of Sciences, Report TR-00-18, Ulaanbaatar, Mongolia.

Amarsaikhan, D., Ganzorig, M., Batbayar, G., Narangerel, D., and Tumentsetseg, Sh., 2004. An integrated approach of optical and SAR images for forest change study. *Asian Journal of Geoinformatics*, No.3, 2004, pp. 27-33.

Amarsaikhan, D., and Douglas, T., 2004. Data fusion and multisource data classification. *International Journal of Remote Sensing*, No.17, Vol.25, pp. 3529-3539.

BEST, 2005. User Manual, Version 4.0.2.

ENVI, 1999. User's Guide, Research Systems.

ERDAS, 1999. Field guide, Fifth Edition, ERDAS, Inc. Atlanta, Georgia.

Gonzalez, R. C. and Woods, R. E., 2002. *Digital Image Processing*. 2nd ed. Upper Saddle River, New Jersey: Prentice-Hall.

Mather, P.M., 1999. Computer Processing of Remotely-Sensed Images: An Introduction, 2nd edition (Wiley, John & Sons).

Mongolian Statistical Year Book, 2005. National Statistical Office of Mongolia, Ulaanbaatar, Mongolia.

Richards, J.A., 1993. Remote Sensing Digital Image Analysis- An Introduction, 2nd edition (Berlin: Springer-Verlag).

Weydahl, D.J., 2001. Analysis of ERS SAR coherence images acquired over vegetated areas and urban features. *International Journal of Remote Sensing*, 22, 2811-2830.